Viscosity enhancement in dilute magnetorheological fluids through magnetic perturbations

F. Donado
Instituto de Ciencias Básicas e Ingeniería de la Universidad Autónoma del Estado de Hidalgo-AAMF, Pachuca 42184, Pachuca, México,
e-mail: fernando@uaeh.edu.mx

U. Sandoval and J.L. Carrillo
Instituto de Física de la Universidad Autónoma de Puebla, Apartado Postal J-48, Puebla 72570, Puebla, México.

Recibido el 7 de febrero de 2011; aceptado el 8 de agosto de 2011

The influence of a sinusoidal magnetic field on the effective viscosity of a magnetorheological dispersion in the low particle concentration regime is studied experimentally. When a sinusoidal magnetic field of low amplitude, conceived as perturbation, is applied transversally to the static field, a significant enhancement occurs in the measured effective viscosity. The magnitude of changes depends on a number of factors such as the amplitude and frequency of the perturbation, the particle concentration, the application time of the fields, and the shear rate. It has also been found that the behavior of the effective viscosity as a function of frequency presents a critical behavior. Therefore, an average Mason number is proposed, whose behavior as a function of frequency is similar to that shown by the effective viscosity.

Keywords: Magnetorheological fluid; effective viscosity; magnetic perturbations.

El efecto de un campo magnético senoidal sobre la viscosidad efectiva de una dispersión magneto-reológica en el régimen de baja concentración de partículas es estudiado experimentalmente. Cuando un campo magnético senoidal de baja amplitud, considerado como perturbación, es aplicado transversalmente al campo estíco, ocurre un significativo incremento en la viscosidad efectiva. La magnitud de los cambios depende de factores tales como la amplitud y la frecuencia de la perturbación, la concentración de partículas, el tiempo de aplicación de los campos, y la rapidez de corte. Se ha encontrado que el comportamiento de la viscosidad efectiva como función de la frecuencia presenta un comportamiento crítico. Por lo tanto, un número de Mason promedio es propuesto, cuyo comportamiento es similar al mostrado por la viscosidad efectiva.

Descriptores: Fluido magneto-reológico; viscosidad efectiva; perturbaciones magnéticas.

PACS: 83.80.Gv; 45.70.Qj; 83.60.Np

1. Introduction

Magnetorheological fluids are composites based on magnetic microparticles dispersed in an inert Newtonian oil, preferably of low viscosity. When they are exposed to an external magnetic field, they experience strong and tunable changes in their physical properties. These composite systems undergo transformation from Newtonian fluids to viscoelastic materials [1–5]. The change in the effective viscosity of the fluids can be of several orders of magnitude and the induced yield stress can be as high as 100 kPa [2]. These systems have attracted the interests of applied researchers to design a wide variety of devices such as dampers and clutches. Some mechanical devices are now commercially available in the market [6–9].

To extend the use of devices based on magnetorheological fluids it is necessary, for some applications, to achieve higher changes in the physical properties for a given magnetic field [10]. Some studies are addressed to obtain more responsive soft magnetic microparticles. Since the characteristics of the aggregates determine the changes in the physical properties, the study of the aggregation process and the methods that modified it, have stirred a great interest because they could allow us to control and enhance the physical properties of MR fluids.

In the low particle concentration regime, the presence of a static magnetic field causes a fast axial aggregation of particles forming chain-like clusters oriented in the magnetic field direction [11]. This configuration can be very stable unless the system is under perturbations, in which case the chains usually undergo lateral aggregation and form columns or longer chains. The most studied type of lateral aggregation is that induced by thermal fluctuation in a system composed by Brownian particles [12–14]. Although this lateral aggregation is generally a very slow process, in the long run could produce significant additional changes in the physical properties [2, 15, 16].

Lateral aggregation in a dispersion of non-Brownian particles can be hastened by external perturbations. Reference 2 reports that a sudden increase of pressure, causes a notable increase in yield stress and forms thicker chains, produced by a fast lateral aggregation. Also there is evidence that an abrupt application of an intense static field results in the formation of a relatively more complex structure compared with that generated by the application of a field whose amplitude increases slowly. In this latter situation, the effective viscosity acquires larger values compared with the case of an abrupt field application [17].

Recently, we have shown that the application of a sinusoidal magnetic perturbation of low amplitude, in addition

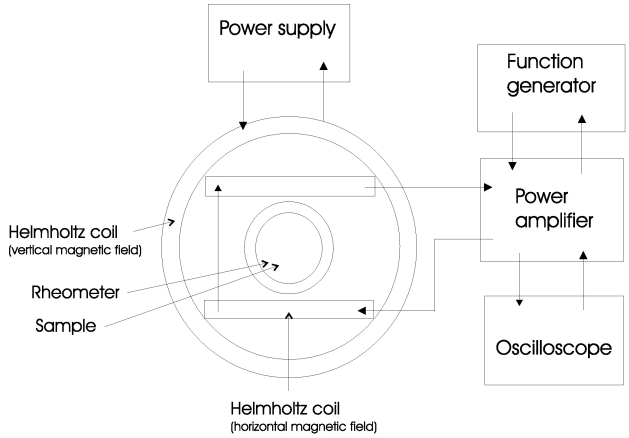

FIGURE 1. Scheme of viscosity setup. The magnetic fields are produced by Helmholtz coils placed perpendicular to each other.

and transversal to the static field, generates significant changes in the average length of the chains formed by particles [15]. This occurs because the chains experience waving movements, they oscillate around the field direction in a path that appears like an "X" shape. By this movement the chains, or more specifically, the end chains, get closer and as a consequence the lateral aggregation is enhanced. Furthermore, the dependence on frequency shows a critical behavior governed by the Mason number. The structure is notably modified by the perturbations that occur in the system. Whether these structural changes can lead to changes in the rheological behavior of the systems has to be found out.

There is no evidence to suggest that similar results occur in the structure of tridimensional system under a low shear rate; however, preliminary rheological results support the fact that perturbation drives notable changes in the rheological behavior of the system. Yet, no general trends can be obtained from them [15, 18]. Now, we present a comprehensive discussion about the effects of the perturbations on the effective viscosity of a magnetorheological dispersion. Specifically we found the critical behavior of the reduced viscosity as a function of frequency. We discuss a method to obtain the average of the Mason number whose behavior is qualitatively similar to that found for reduced viscosity.

2. Viscosity measurements

The samples were prepared by dispersing magnetite particles in Dexron oil; the particles have an average size of 65 μm and a standard deviation of 15 μm. The particle concentration is indicated by the fraction of volume occupied by the particles, ϕ; in most cases $\phi = 0.05$. To measure the effective viscosity in the MR fluid samples, we used a Brookfield LVDV-III cone-plate viscometer. The temperature of the samples was kept constant at 20°C by using a Brookfield TC 602P thermal bath. The static field was applied in the vertical direction, and as a perturbation, a sinusoidal field was applied in the horizontal direction. In most of the experiments presented in this work, the amplitude of the static field

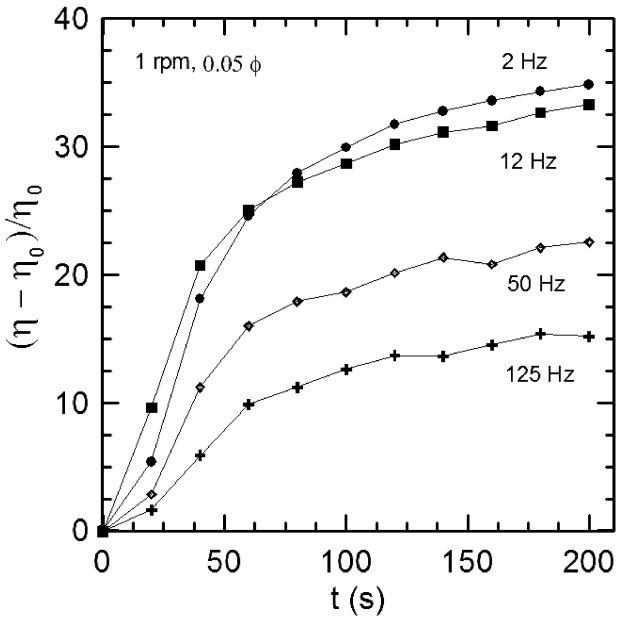

FIGURE 2. Reduced viscosity as a function of time for different frequencies of the perturbation.

was 80 G and the sinusoidal field was 17 G whose root mean square represents the 15% of the static field. The magnetic fields were generated by means of two couples of Helmholtz coils. The recipient that contained the sample was made of a nonmagnetic material. The cone and plate were 3 mm apart; it allowed the formation of chains of different lengths. Figure 1 shows a diagram of the experimental setup.

The measurements have two stages. In the first one, we measure the effective viscosity of the dispersion with no applied fields, η_0, across a time interval of 200 s. This pretreatment of the sample is to avoid inhomogeneity in the dispersions and variations in the value of the effective viscosity without field. Then both fields, the static H_b and the perturbation H_p are applied and the effective viscosity is taken every 10 s during a span of 900 s. Although these are only shown as values corresponding to times below 200 s after the fields were turned on, in order to discuss general trends of the effective viscosity in terms of previous results of kinetics of aggregation performed in the same period. The cone of the viscometer rotates at 1 RPM in the experiments, except when it is indicated otherwise. In the graphs is shown the reduced viscosity, $(\eta - \eta_0)/\eta_0$ of the dispersion.

Figure 2 shows a comparison of the time dependence of the reduced viscosity behavior for four cases corresponding to four perturbation frequency values. In this figure we can observe some general trends about the temporal behavior of the reduced viscosity, the trend of the reduced viscosity as a function of frequency is discussed in detail below. We observed that immediately after the fields were turned on, the reduced viscosity increased very fast, approximated during one quarter of the time reported, and after that, the increase was slower. The quick changes in reduced viscosity can be associated with the axial aggregation and the formation of chains; the slower changes instead can be associated with the

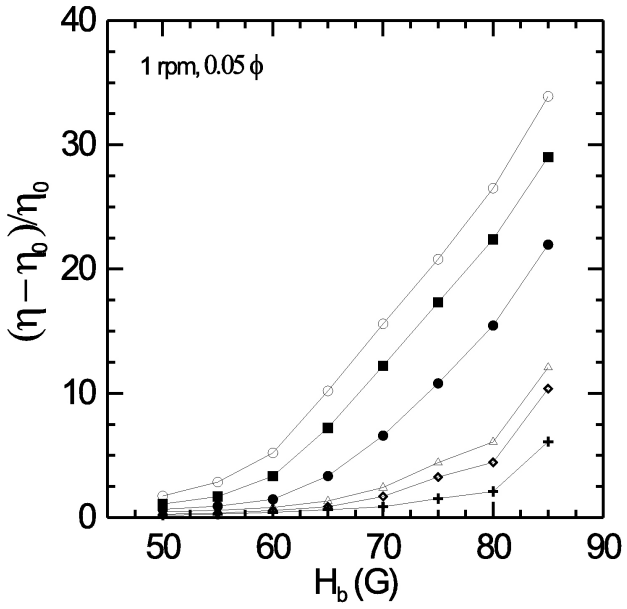

FIGURE 3. Reduced viscosity as a function of the intensity of static magnetic field. The perturbation field remains in 15 % of the static magnetic field. The upper curves correspond to the measurements at three different times; empty circles, 200 s; filled squares, 100 s; dots, 50 s. The lower curves correspond to the case with no perturbation also for different times, open triangles, 200 s; open diamonds, 100 s; and cross, 50 s.

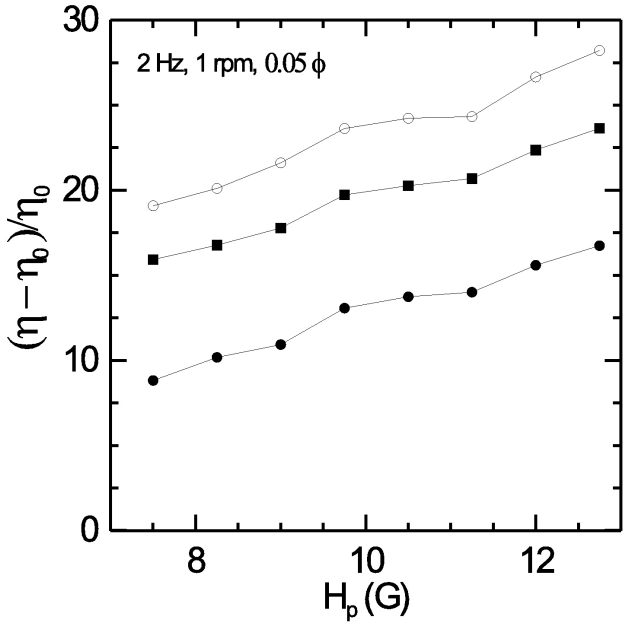

FIGURE 4. The reduced viscosity is measured for eight different values of the perturbation amplitude, maintaining the intensity of the static field constant at $80G$. Again, the curves respectively correspond to the measures taken at 50 s dots, 100 s squares, and 200 s empty circles.

lateral aggregation induced mainly by the effects of the shear rate and the perturbation field. The same trend is observed when it only acts a static field; however, the values achieved by the reduced viscosity are in general lower than when the perturbation is present, *e.g.* at 200 s with a static field of 80 G, the reduced viscosity reaches 7 units in the y-scale of the Fig. 2. We obtained similar curves for several conditions of intensity fields, perturbation frequency, particle concentration, and shear rate; with the values of the reduced viscosity at 50, 100 and 200 s we constructed the curves that show the behavior of the reduced viscosity as a function of intensity of the fields, perturbation frequency, particle concentration, and shear rate. In the graph of the behavior of the reduced viscosity as a function of time of application we considered several times of field applications.

Figure 3 shows the comparison of reduced viscosity when both fields are varied keeping the ratio between them at 15% (three upper curves) with the case without the perturbation field (three lower curves). In the graphs, there are only shown the values of the static field. The dots, the squares, and the empty circles curves are the measurements of reduced viscosity taken at 50 s, 100 s, and 200 s, respectively. It is clear that the perturbation induces noticeable changes in the reduced viscosity. The physical reason behind this notorious change in the reduced viscosity, is that when the perturbation is applied the lateral movements induced by the perturbation act over the chains and the lateral aggregation is enhanced. This mechanism of induced lateral aggregation produces thicker and larger clusters leading to larger values of the reduced viscosity. This aggregation mechanism does not exist in the absence of the perturbation field; consequently, the growing rate of the reduced viscosity in this latter case is smaller.

Figure 4 shows the behavior of the reduced viscosity as a function of the amplitude of the perturbation field. The amplitude of the static field is fixed at 80 G. As expected, at least for the measurements taken at 50 s, 100 s, and 200 s the reduced viscosity acquires larger values for larger amplitudes of the perturbation field. Larger amplitude of the perturbation means the amplitude of the lateral movements of the extremes of the chains are larger, the chain ends sweep a larger area around them, and the possibility to interact with other chains is increased and for that reason the lateral aggregation grows with the amplitude. However, the amplitude must be small, lower than 25% of the static field, because larger amplitudes produce chain ruptures.

Figure 5 shows the dependence of reduced viscosity on perturbation frequency. Frequency of the perturbation field was varied in a wide interval for two values of the static field, 80 G and 70 G, keeping the ratio $(\mathrm{H}_p/\sqrt{2})/\mathrm{H}_b$ at 15%. Certain facts of the two graphs must be emphasized. The first one is the existence of a maximum in the reduced viscosity as a function of the frequency. It means that the frequency of the perturbation can also be used to control the effective viscosity. The second fact is that, for these values of the applied fields, the maximum values obtained by the reduced viscosity (marked with an arrow) are reached for different frequencies, 3.6 Hz for 80 G and 2.6 Hz for 70 G. There is a shift to higher frequencies for larger values of the intensity of applied fields. This phenomenon can be understood on the basis of the kinetics of aggregation as follows: For higher values of the ap-

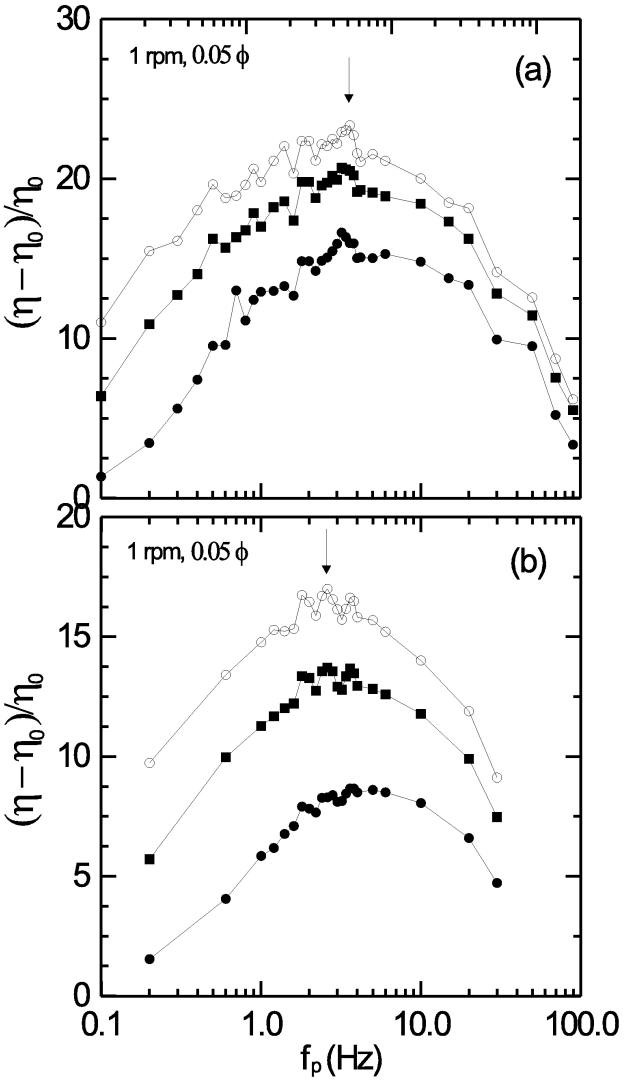

FIGURE 5. The reduced viscosity as a function of perturbation frequency keeping the intensity of the static field at (a) 80 G and (b) 70 G. The curves correspond to the measurements taken at 50 s, dots; 100 s, squares; and 200 s, empty circles.

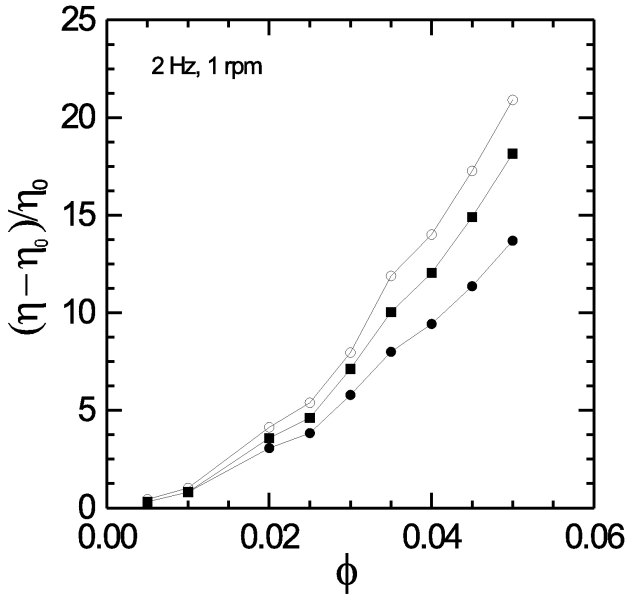

FIGURE 6. The reduced viscosity as a function of the particle concentration. The curves respectively correspond to the measures taken at 50 s dots, 100 s squares, and 200 s empty circles.

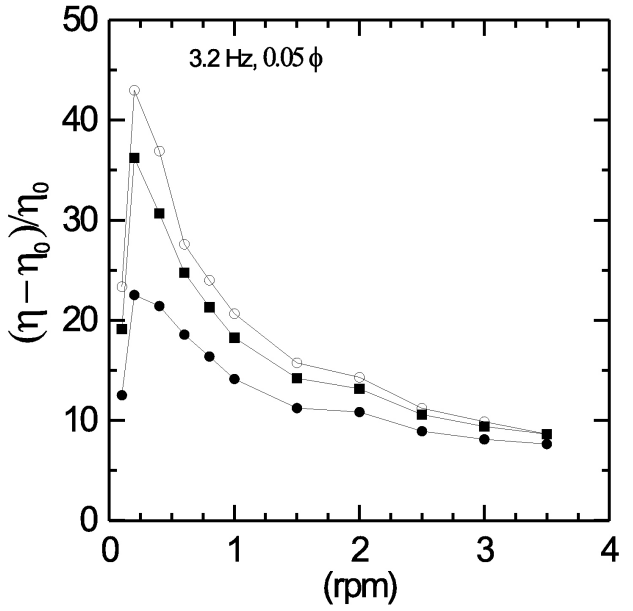

FIGURE 7. The reduced viscosity as a function of the revolutions per minute of the viscometer cone. The curves respectively correspond to the measures taken at 50 s dots, 100 s squares, and 200 s empty circles.

plied field the magnetic bonding between particles is stronger, for that reason the maximum appears to higher frequencies. The existence of a maximum value can be understood because at higher frequencies of the field the chains do not respond as fast to follow the fields. The values indicated by arrows, where the reduced viscosity has a maximum coincide quite well with the recently predicted values on the basis of kinetics of aggregation [15].

The particle concentration is, of course, another of the important variables that is anticipated to influence notoriously the effective viscosity. It is a reasonable expectation that for larger values of the particle concentration the applied fields might generate more and thicker chains, leading to larger values of the effective viscosity. Figure 6 corroborates this intuitive expectation. It shows a series of measurements of the reduced viscosity as a function of the particle concentration ϕ. The values of the other external parameters are specified in the graph. Here the applied static field is set to 80 G with the ratio between $\mathrm{H}_p/\sqrt{2}$ and H_b being 15%. The measurements presented correspond to 50 s, 100 s, and 200 s, for nine values of the particle concentration, measured in volume fraction. Larger concentrations were not studied, but it is expected the reduced viscosity reaches a maximum and after that it decreases as the concentration grows. The decreasing behavior that is expected in the high concentration regime is because while $\eta - \eta_0$ decreases, η_0 increases very fast as the concen-

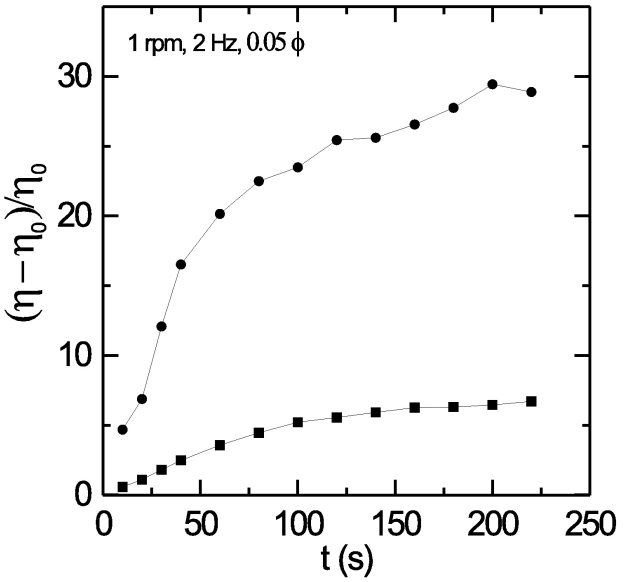

FIGURE 8. The upper curve corresponds to the reduced viscosity as a function of the time of application of the perturbation field. The lower curve corresponds to the case when no perturbation field was applied and also for different times of the application of the field.

tration enhances [19]. The difference $\eta - \eta_0$ decreases as the concentration enhances because the structural changes, induced by the magnetic field, decrease as particles are increasingly close to each other.

Figure 7 contains the results of reduced viscosity as a function of revolutions per minute (RPM) of the cone of the viscometer. It is observed that for small RPM the aggregation process is more effective to enhance the effective viscosity than for higher RPM. In this latter case, the hydrodynamic forces contribute to break the magnetic bindings between the particles in the chains, resulting in the high shear stress, a limiting mechanism for the effective viscosity.

Figure 8 shows the behavior of the reduced viscosity as a function of the time of application of the perturbation field. The experiments were conducted as follows: The static and the perturbation fields were simultaneously applied to the sample. After some time of application the perturbation field was turned off, but the static field was continued. The enhancement of the reduced viscosity stops and reaches almost a stationary reduced viscosity value; these values are shown in the graph. The results indicate that perturbations produce an internal rearrangement of the structure and increase the effective viscosity and these changes are stable. These observations evidence the point that it is not necessary to apply the perturbation all the time to increase the effective viscosity. It is only necessary to apply it for a period of time.

3. Frequency critical behavior and the Mason number

As we observed from the above experimental results the reduced viscosity as a function of the frequency of the perturbation presents a critical behavior. For example, when the static field is 80 G the reduced viscosity increases as the frequency grows until the reduced viscosity reaches a maximum value at arround 3 Hz; for higher frequencies the reduced viscosity decreases. Based on studies of dispersions of magnetic particles in viscous liquids under magnetic fields where the particles move through the liquid [20–22], we can propose that the critical behavior found for the reduced viscosity as a function of the frequency is governed by the Mason number. The Mason number $\widetilde{Ma}$ is the ratio between the magnitudes of viscous force and magnetic force that act over a pair of particles. It determines the dynamics of the aggregates of particles and the behavior of the physical properties. If $\widetilde{Ma} = 1$, the system usually presents a critical behavior. When the magnetic force dominates over the viscous force, then $\widetilde{Ma} < 1$; the system has a behavior that is qualitatively different from others when the viscous force surpasses the magnetic force, $\widetilde{Ma} > 1$.

In our system the particles formed chains that oscillated around the static field due to the oscillating effect of magnetic field. As they move they have a variable angular frequency and therefore a time-dependent Mason number. Since the Mason number governs the dynamics of the system we attempt to find a function of the Mason number that has the same general trend as the reduced viscosity.

In the following paragraphs of the section we describe how we obtain the Mason number in the case of rotating field, then we analyze numerically an equation for the phase lag and the angular position described by the chains; based on this analysis we propose a method to average the Mason number in our system that let us propose a function whose behavior is comparable to the reduced viscosity.

To evaluate the Mason number for a pair of joined particles in a rotating magnetic field, we need to determine the magnetic force between the particles and the viscous force due to the liquid. First we obtained the magnetic force. Let us consider a system of particles under a magnetic field, where each particle behaves as a magnetic dipole whose dipolar moment induced by the magnetic field is

$$\vec{m} = \frac{4\pi R^3}{3}\vec{M},$$

where $\vec{M}$ is the magnetization and R the radius of the particles. The magnetization and the effective magnetic field are related through the formula $\vec{M} = \chi_p \vec{H}$, where χ_p is the magnetic susceptibility. A magnetic dipole $\vec{m}_1$ exerts a magnetic force over a dipole $\vec{m}_2$ at a position $\vec{r}$ given as

$$\vec{F} = -\nabla U(\vec{r}), \tag{1}$$

where $U(\vec{r})$ is given by

$$U(\vec{r}) = -\vec{m}_2 \cdot \vec{H}(\vec{r}), \tag{2}$$

where $\vec{H}(\vec{r})$ is the magnetic field generated by $\vec{m_1}$ and whose expression is [23]

$$\vec{H}(\vec{r}) = \frac{\mu_0}{4\pi}\left(\frac{3\vec{r}\cdot\vec{m}_1}{r^5}\vec{r} - \frac{\vec{m}_1}{r^3}\right). \tag{3}$$

If both dipoles are oriented in the same direction the magnetic force between the particles is given as

$$\vec{F}_{\text{mag}} = \frac{3\mu_0}{4\pi}\left[\left(\frac{m^2}{r^5} - \frac{5(\vec{r}\cdot\vec{m})^2}{r^7}\right)\vec{r} + \frac{2(\vec{r}\cdot\vec{m})}{r^5}\vec{m}\right]. \quad (4)$$

If now we use the fact that the particles are joined to form a pair oriented in the direction of the field and we write the dipolar moment in terms of the magnetization, the magnetic force is derived as follows:

$$F_{\text{mag}} = \frac{\mu_0\pi R^2 M^2}{6}. \quad (5)$$

Now we obtain the viscous force over the pair. For a sphere of radius R that moves at a relative speed $\vec{V}$ in the liquid this interaction is

$$\vec{F}_{\text{vis}} = -6\pi\eta R\vec{V}. \quad (6)$$

The maximum tangential speed V for each particle, considering that it rotates around the junction point at the angular frequency ω of the rotation field, is $\omega(2R)$, thus the viscous force over the pair is given by

$$F_{\text{vis}} = -2(6\pi\eta R\omega(2R)), \quad (7)$$

Therefore, the Mason number for this system [22], the ratio between the magnitudes of the viscous force and the magnetic force, is as follows:

$$\widetilde{Ma} = \frac{12^2\eta\omega}{\mu_0 M^2}. \quad (8)$$

The Mason number can also be obtained from the motion equation of a pair of particles in a rotational field of frequency ω when it was written in terms of the dimensionless distance between particles centers, $\rho \equiv r/2R$, and the dimensionless time $\tau \equiv t/t_s$, where $t_s = 12^2\eta/\mu_o M^2$. The Mason number arises as a dimensionless frequency given by $\widetilde{Ma} = t_s\omega$.

In the literature different forms had been proposed to model the dynamics of magnetic particles in rotational fields. We have based on the proposal given in Ref. 24 for angular position of axisymmetric particles ψ with respect to some fixed direction, where instead of using the frequency of the rotating field we use the Mason number since it can be considered as a dimensionless frequency. Thus, we propose the equation to model ψ of a pair of particles that are joined is given by

$$\frac{\mathrm{d}\psi}{\mathrm{d}\tau} = \frac{MH}{\alpha}\sin(\widetilde{Ma}\tau - \psi), \quad (9)$$

where α is the rotational friction coefficient. This equation can be rewritten using the phase lag β between the field and the angular position of the pair of particles, $\beta \equiv \widetilde{Ma}\tau - \psi$ [24]

$$\frac{\mathrm{d}\beta}{\mathrm{d}\tau} = \widetilde{Ma} - \widetilde{Ma}_c\sin(\beta). \quad (10)$$

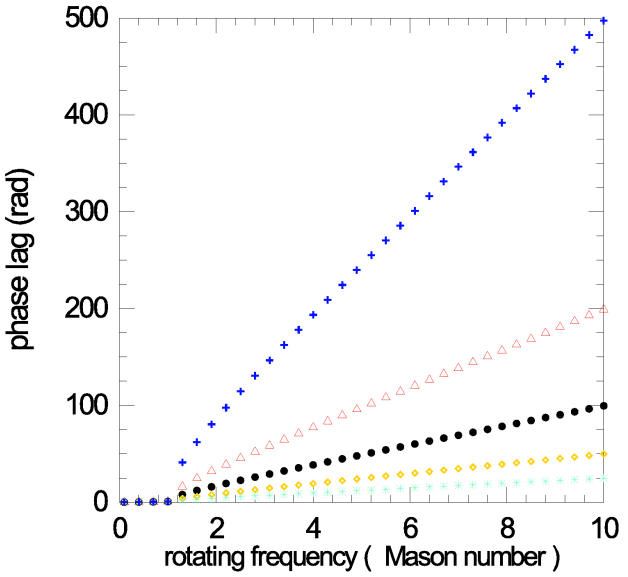

FIGURE 9. Phase lag orientation as a function of the Mason number for different simulation times (in dimensionless time units τ); crosses, 100 τ; triangles, 40 τ; dots, 20 τ; diamonds, 10 τ; stars, 5 τ.

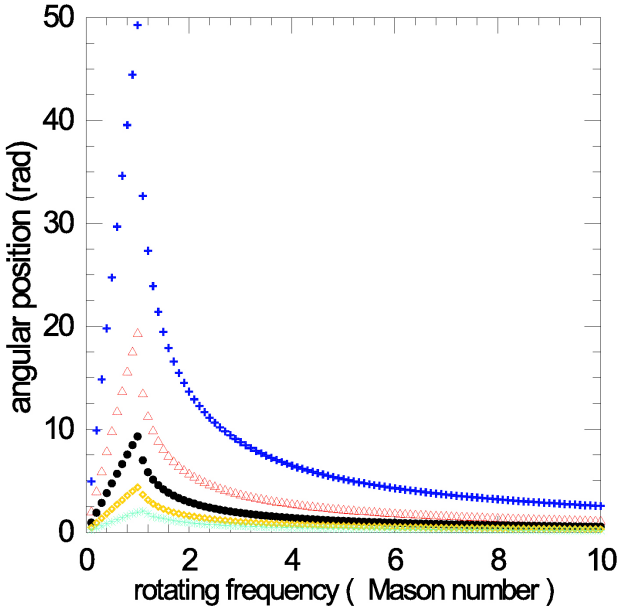

FIGURE 10. Angular position as a function of the Mason number for different simulation times (in dimensionless time units τ); crosses, 100 τ; triangles, 40 τ; dots, 20 τ; diamonds, 10 τ; stars, 5 τ.

In Fig. 9 we observe the behavior of the phase lag of a pair of particles as a function of Mason number for different simulation times τ. It is worth noticing that when Mason number equals one there is a critical behavior. The phase lag values when $\widetilde{Ma} < 1$ are low and change slowly; however, when $\widetilde{Ma} > 1$, the phase lag increases very fast. This means that when $\widetilde{Ma} < 1$ the pair of particles moves synchronously with the field, and when $\widetilde{Ma} > 1$ the pair of particles no longer follows the field, and they are delayed in relation to

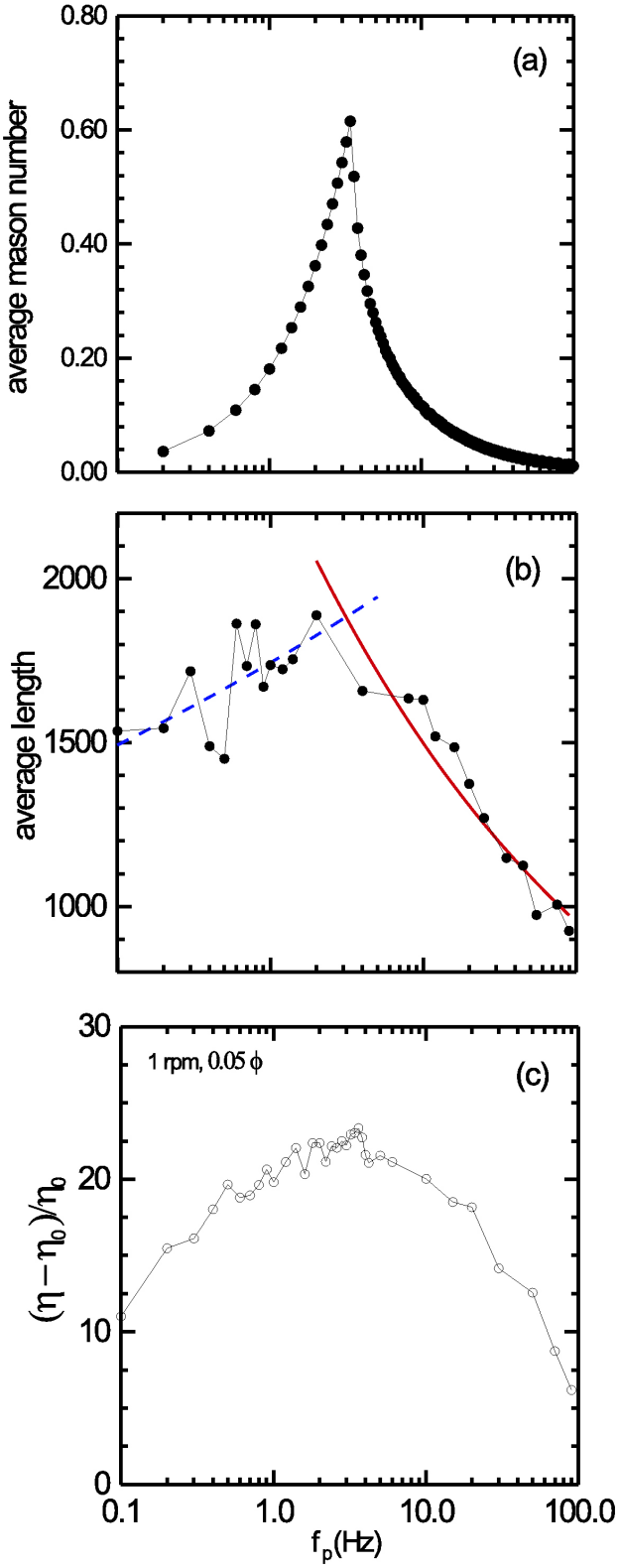

FIGURE 11. (a) Average mason number, (b) average length of the chains, and (c) reduced viscosity, all curves as a function of the perturbation frequency, the maximum values occur at 3.4 Hz, 3.1 Hz and 3.6 Hz, respectively.

the field orientation. This behavior would be reflected in the angular position. Figure 10 shows the behavior of the angular position of the pair of particles ψ as a function of the Mason number, the curves correspond to the same conditions for the phase lag curves in Fig. 9 and have been obtained through the formula, $\beta \equiv \widetilde{Ma}\tau - \psi$. It is observed that for $\widetilde{Ma} < 1$ the average angular position is increasing as the frequency increases; however, if $\widetilde{Ma} > 1$ the amplitude decreases as the frequency increases. It is observed that the decline of the amplitude of the angular position is very fast around the critical frequency.

Now we can come back to our system exposed to an effective oscillating field given as

$$\vec{H}_{ef} = \left[H_c\hat{i} + H_p \text{sen}(2\pi f_p t)\hat{j}\right], \tag{11}$$

where the static magnetic field direction determines the x-axis, H_c is the static field intensity and H_p the amplitude of the sinusoidal field, considered as perturbation, with frequency f_p. This effective magnetic field oscillates around the direction defined by the static field and forms an angle given by

$$\psi = \psi_{\text{max}} \text{sen}(2\pi f_p t), \tag{12}$$

where ψ_{max} is the maximum angle formed by the effective magnetic field direction and the static field direction, it is obtained from $\psi_{\text{max}} = \tan^{-1}(H_p/H_c)$. For $H_c = 80$ G and $H_p = 17$ G, values used in the work, $\psi_{\text{max}} = 0.20$ rad.

During the oscillation the chains describe an angle given by Eq. 12. When the chain follows the direction of the magnetic field, the angular speed can be obtained from Eq. 12, that is

$$\omega = 2\pi f_p \psi_{\text{max}} \cos(2\pi f_p t). \tag{13}$$

As it is observed the angular speed is a function of time. If the expression 8 is taken as base, the Mason number for our system can be expressed as,

$$\widetilde{Ma} = \frac{12^2 \eta \left(2\pi f_p \psi_{\text{max}} \mid \cos(2\pi f_p t) \mid\right)}{\mu_0 M^2} \tag{14}$$

where f_p is the perturbation field frequency, M is the particle magnetization and η is the liquid viscosity. We can observe that the Mason number in our case is a time dependent function. In this expression we consider only the absolute value of the cosine function in order to keep the Mason number as the ratio between the magnitudes of forces. The simple averaging of this expression of the Mason number does not present a critical behavior; it is a linear function. Based on results from rotating fields we can propose that in the case of time-dependent field, the evolution of the dynamics of the chains are governed mainly by the intervals where the Mason number is below unity. When $\widetilde{Ma} < 1$, the chains follow the direction of the magnetic field synchronously and with a small phase lag, the resulting waving movements promote lateral aggregation. However in the intervals where $\widetilde{Ma} > 1$, the chains are no longer in phase with the field direction, and the waving movements are damped, their effectiveness to drive

lateral aggregation is reduced. Therefore, when a sinusoidal perturbation is present its effectiveness to enhance lateral aggregation depends on how much the chains move under the condition $\widetilde{Ma} < 1$ during the time in consideration. In accordance with this, we proposed an average Mason number where only the differential contributions where $\widetilde{Ma} < 1$ are computed for the integral evaluation of the average, that is

$$\bar{Ma} = \frac{1}{T}\int_0^T \kappa \widetilde{Ma} dt \tag{15}$$

where $\kappa = 0$ if $\widetilde{Ma(t)} > 1$ and $\kappa = 1$ if $\widetilde{Ma(t)} \leq 1$; T is the perturbation period.

The defined integral, evaluated for several frequencies, where the magnetization and viscosity are obtained elsewhere [15], gives the graph shown in the Fig. 11(a). It is observed that the behavior of this average Mason number presents some similarities with aggregation and effective viscosity results. First, it shows a critical behavior around the perturbation frequency 3.4 Hz. This value is close to the corresponding value in aggregation experimental results [15], 3.1 Hz, see Fig. 11(b) and from effective viscosity results shown before, 3.6 Hz, and repeated in Fig. 11(c). Second, it presents also, for the left hand side with respect to the critical behavior, an increasing behavior and for the right hand side, decreasing one. However there is an evident difference among them; the concavity of this average Mason number is not as those present in experimental results. Similarly, the qualitative relation can be improved by adding the effects of more variables.

4. Comments and remarks

The aim of this work was to characterize the effective viscosity behavior of an MR fluid under the influence simultaneously of a static magnetic field and a sinusoidal field conceived as a perturbation.

The effective viscosity behavior of the system shows a notable dependence on the perturbation field. The origin of this behavior is the restructuring of the chains due to the oscillating effective field. Although we have not carried out a study of the kinetics of aggregation in a tridimensional system under shear, the present study shows the general trends observed on rheological behavior are similar and are in accord with results of the kinetics of aggregation studies on a 2-dimensional system. Specifically, the frequency dependence in both rheological and structural studies are very close. It supports the hypothesis that the kinetic mechanism of aggregation induced by the perturbation acts in a 3-dimensional system under low shear rate as well as in a 2-dimensional system. It enhances the lateral aggregation, producing larger and thicker chains in the structure in a way remarkably more intense and faster than that produced only by thermal fluctuations and these changes produce rheological changes.

In summary, the results discussed here indicate that in the regime of low particle concentration, by controlling the amplitude and frequency of the magnetic perturbation it is possible to perform a dynamical manipulation of the rheological response of a MR fluid. One could expect that by properly scaling the characteristic of the applied fields, most of the results here discussed would occur similarly in an MR fluid composed by smaller particles; of course, in that case thermal fluctuations also would be considered. An analogous behavior would also happen in electrorheological fluids.

Acknowledgments

The study was supported financially by CONACyT México, Grant No. 80629. U. Sandoval acknowledges the CONACyT fellowship.

1. D. Kittipoomwong and D. Klingenberg, *J. Rheol.* **49(6)** (2005) 1521.
2. R. Tao, *J. Phys.: Condens. Matter.* **13** (2001) R979.
3. J. Vicente, M.T. López-López, J.D.G. Duran and F. Gonzalez-Caballero, *Rheol. Acta* **44** (2004) 94.
4. G.K. Auernhammer, D. Collin, and P. Martinoty, *J. Chem. Phys.* **124** (2006) 204907.
5. P. Domínguez-García, S. Melle, and M.A. Rubio, *J. Colloid Interface Sci.* **333** (2009) 221.
6. A.G. Olab y A. Grunwald, *Materials and Design* **28** (2007) 2658.
7. http://www.lord.com/Home/ MagnetoRheologicalMRFluid/ tabid/3317/Default.aspx
8. T. Gerlach, J. Ehrlich, and H. Bse, *Journal of Physics: Conference Series* **149** (2009) 012049.
9. A. L. Browne, J. D. Mccleary, C.S. Namuduri, and S.R. Webb, *Journal of Intelligent Material Systems and Structures* **20** (2009) 723.
10. X.Z. Zhang, X.L. Gong, P.Q. Zhang, and Q.M. Wang, *J. Appl. Phys.* **96** (2004) 2359.
11. P. Domínguez-García, S. Melle, J.M. Pastor, and M.A. Rubio, *Phys. Rev. E* **76** (2007) 051403.
12. E.M. Furst and A.P. Gast, *Phys. Rev. E.* **62** (2000) 6916.
13. J.E. Martin, *Phys. Rev. E.* **63** (2000) 011406.
14. S. Cutillas and J. Liu, *Phys. Rev. E* **64** (2001) 011506.
15. F. Donado, U. Sandoval, and J.L. Carrillo, *Phys. Rev. E* **79** (2009) 011406.
16. J.E. Martin, K.M. Hill, and C.P. Tigges, *Phys. Rev. E* **59** (1999) 5676.
17. M. Chaker, N. Breslin and J. Liu, *Proc. 7th. Int. Conf. on ER*

Fluids and MR Suspensions Ed. R Tao (World Scientific, Singapore, 2000) pag. 366

18. U. Sandoval, J.L. Carrillo, and F. Donado, *Rev. Mex. Fís. E* **56**(1) (2010) 123.
19. R.G. Larson, *The Structure and Rheology of Complex Fluids*, 1st Ed. (Oxford University Press, New York, 1999) Chap. 6.
20. S. Melle, and J.E. Martin, *J. Chem. Phys.* **118** (2003) 9875.
21. O. Volkova, S. Cutillas, and G. Bossis, *Phys. Rev. Lett.* **82** (1999) 233.
22. S. Melle, O.G. Calderon, M.A. Rubio, and G.G. Fuller, *Phys. Rev. E* **68** (2003) 041503.
23. J.R. Reitz, F.J. Milford, and R.W. Christy, *Fundations of Electromagnetics Theory*, 3nd. Ed. (Addison-Wesley Publishing Company, Massachusetts, 1979) Chap. 8.
24. A. Cebers and M. Ozols, *Phys. Rev. E* **73** (2006) 021505.